Electromagnetic Priming of Ceramic Foam Filters (CFF) for Liquid Aluminum Filtration

Robert Fritzsch[1], Mark William Kennedy[1,2], Jon A. Bakken[1], Ragnhild E. Aune[1,3]

[1]Department of Materials Science and Engineering, Norwegian University of Science and Technology, N-7491 Trondheim, NORWAY
[2]Proval Partners S.A., 70 Rue de Genève, 1004 Lausanne, SWITZERLAND
[3]Department of Materials Science and Engineering, Royal Institute of Technology, 100 44 Stockholm, SWEDEN
Communicating author: ragnhild.aune@ntnu.no

Keywords: Priming, Electromagnetism, CFF, Aluminum

Abstract

Commercial Ceramic Foam Filters (CFF) of 30, 50 and 80 Pores Per Inch (PPI) have been primed, using magnetic field strengths of 0.06-0.2T, for periods of 1-10 minutes. The influence of time and field strength on the gas removal from the CFF structure, and the resulting improvements in filter productivity, are discussed. The obtained results are related to Finite Element Modeling (FEM) of the metal flow fields induced by the electromagnetic Lorentz forces. Higher filtration rates were obtained for 50 PPI magnetically primed, than for 30 PPI gravity primed filters. This suggests that electromagnetic priming offers an opportunity to use 50 PPI filters, with a higher overall filtration efficiency than 30 PPI filters, in existing cast house applications where the low productivity/high priming head of these filters would otherwise rule them out. Estimated filtration efficiency of different filter types are presented as functions of velocity and thickness.

Introduction

Aluminum melts contains a large number of inclusion particulates of ≤ 50 µm in size. These inclusions may be particles, bifilms or clusters of: oxides (Al_2O_3, SiO_2), spinels ($MgO \cdot Al_2O_3$), carbides (SiC, Al_4C_3), nitrides (AlN), borides (TiB_2), sulfides, phosphides and intermetallics [1]. Large concentrations or inclusions over critical size limits can render metal un-fit for purpose and result in serious financial consequences for metal producers. Inclusions in the aluminum melt can have a negative impact on the machinability, mechanical properties, and can lead to increased gas porosity and shrinkage of the material during casting [1]. Higher utilization of post-consumed and process aluminum scrap will increase the potential for melt contamination by inclusions and result in greater challenges to achieve both metal yield and the required quality standards. These challenges can be expected to increase in the future.

The aluminum industry has developed a number of treatment processes to improve metal cleanliness. CFFs are the most commonly applied filtration process and have been used to filter >50% of the world production of aluminum since the 1990's [2].

Recently the impact of electromagnetic fields generated by solenoidal coils on the filtration of SiC inclusions with CFFs has been a subject of experimental study. Batch filtration experiments [3, 4] to investigate the impact of the electromagnetic (EM) field on metal flow inside the filter and flow filtration experiments to determine the quantitative filtration efficiency [5] have been conducted with 30, 50 and 80 PPI CFFs. The particle sizes in the recent experiments were small, the particles were well wet by the aluminum (unlike alumina or bifilms) and the concentration was extremely high; hence, the measured filtration efficiency is not directly comparable to industrial conditions. The focus of this paper is therefore on measured priming behavior and not experimental filtration efficiency. Filtration efficiency will be discussed on the basis of published filtration models for 'normal' particles in standard alloys, and for commercially significant casting velocities.

Theory

Electromagnetic priming was discovered during early development work and is the subject of a recent US patent application [6]. It has been found that in the presence of an AC magnetic field, CFFs of 30-80 PPI can be primed without preheating, while using only 100-150 mm of metal head. This simple and highly effective procedure will be described in further detail in this paper and the possible implications for the commercial filtration process discussed.

Helical induction coils have been combined with standard Ceramic Foam Filters (CFFs) in recent experiments in order to study the impact of electromagnetic Lorentz forces on the filtration of liquid aluminum, as shown in Figure 1 [5]. An alternating current (50 Hz) was applied to the coil in the phi-direction, which produced a time varying magnetic flux density, B_z [T] along the vertical z-axis of the apparatus. The time varying magnetic field induced currents, J_ϕ [A/m^2] in the liquid metal over, inside and under the CFFs, in a direction opposing the current applied

to the coil (negative phi-direction). Electromagnetic Lorentz forces, F_r [N/m^3] were produced by the interaction of the flux density and the induced current density, according to the cross product (in the negative r-direction):

$$F_r = J_\phi \times B_z \qquad [1]$$

A gradient exists in the flux density along the z-axis of real, i.e. 'short' coils [3], which in turn leads to a gradient in the induced current. These two gradients combine to make a significant gradient and curl in the induced Lorentz forces. The curl is further accentuated by the differences in the electrical conductivity in the filter region [4], causing powerful magneto-hydrodynamic mixing (MHD) effects to be created. The effective conductivity of the metal within the CFF, is reduced due to the tortuosity and porosity of the filter [7]. Lorentz forces and the resulting MHD flow fields will be presented based on the output from a COMSOL® 2D axial symmetric finite element model (FEM). The validation of the COMSOL® induction heating/magnetic field model has been published elsewhere [8-10].

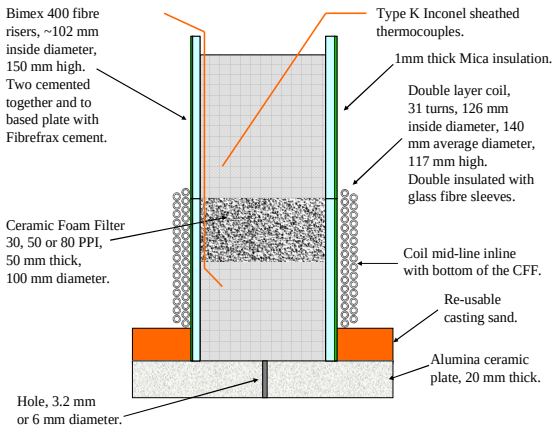

Figure 1. Schematic of the experimental apparatus used for filtration experiments. The mid-line of the coil and highest flux density is in line with the bottom of the CFF [5].

Experimental Methods and Materials

Experiments (12) were recently conducted using 150 kg batches of melt, for 4 experiments of up to 25 kg each. The charge was mixed and melted in a graphite agitated resistance furnace with a target temperature of 1023 K. The melt recipe was 90% A356 alloy, and 10% A356 composite master alloy, which reportedly containing 15 wt. % SiC particles, with a size range of 13-23 µm. The detailed experimental procedures have been described elsewhere [3, 5].

The filters were primed electromagnetically for 6 minutes at the start of each the EM experiments. A current of approximately 730 A was applied to the 31 turn induction coil (shown in Figure 1) and aluminum was added to the apparatus without preheating of the filter element. The electromagnetic field was active while pouring of the melt into the crucible. During the priming, the metallic head was kept relatively constant at ~150 mm. A maximum head of 150 mm was sufficient to prime 30, 50 and 80 PPI filters in all cases. After priming a discharge hole was opened in the bottom of the alumina plate for subsequent filtration efficiency measurements, as shown in Figure 2. Flow rate during filtration was determined by gain-in-weight on the receiving vessel and weightometer shown in Figure 2.

Electromagnetic priming has also been explored via batch experiments using:

- Different coil configurations (single and double layer),
- Various magnetic flux densities (0.06-0.2 T),
- Various test durations (1-10 minutes), and
- Filter types (30, 50 and 80 PPI).

Experiments using gravity priming for 30, 50 and 80 PPI have also been conducted.

Figure 2. Experimental apparatus for the flow filtration experiments, showing aluminum metal being added continuously via a ladle and discharging into a receiving vessel placed on a weightometer [5].

Priming and wetting

CFF's are normally operated in a "filter bowl" and are primed using a gravity head of liquid metal with a recommended pre-heating procedure [11]. The gravity head forces the metal into and through the CFF, displacing much of the interstitial air. The poor wetting characteristics of alumina by aluminum and the need to remove air can lead to difficulties at the start of the filtration process, particularly with high pore density filters. The typical magnitudes of industrial priming heads are plotted in Figure 3 for different grades of commercial filters [12, 13].

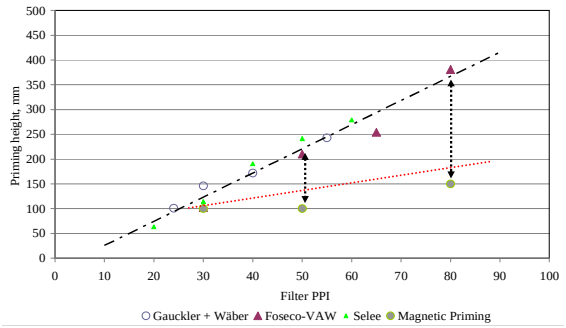

Figure 3. Priming height vs. filter PPI from different producers compared with electromagnetic priming at ~0.17 T [12, 13]. 30 PPI filters could have been primed with less than 100 mm of metal head, as indicated by the dotted red line.

Photographic images of the (a) 50 and (b) 80 PPI CFFs after a gravity priming experiments using 100 mm metal head, are shown in Figure 4. The filters failed to prime, as had been fully expected based on Figure 3. The molten metal solidified over the filter elements with nearly complete lack of penetration of metal into the filters. The filters have been removed, showing the 7-18 mm of penetration, i.e. the small amount of CFF remaining attached to the underside of the frozen metal.

Repeating the experiments in the presence of an electromagnetic field (~0.17 T), results in complete filter priming, with the same initial 100 mm of metal head as indicated for (a) 50 PPI and (b) 80 PPI CFF in Figure 5. 150 mm of head is recommended for 80 PPI CFFs as shown in Figure 3, based on experiences over many batch and flow experiments, to ensure rapid metal penetration without requiring excessive initial metal superheat.

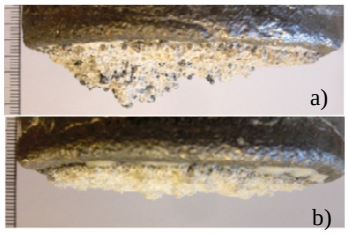

Figure 4. 'Unsuccessful' gravity experiments with 150 mm of head showing metal frozen over the filter with: (a) ~18 mm of metal penetration, using a 50 PPI CFF and (b) less than 7 mm of metal penetration, using a 80 PPI CFF.

The vertical filter sections Figures 5 (a) and (b), show improved filter wetting, as well as successful removal of most gas after only 3 minutes of electromagnetic priming. This can be better observed in the SEM micrographs (c) 50 PPI and (d) 80 PPI, after 10 minutes of electromagnetic priming.

Additional experiments have successfully primed stacks of (3) 30, 40, 50 and 80 PPI CFFs, with a metal head of 150 mm using an ~0.17 T electromagnetic field and the same coil pictured in Figures 1 and 2.

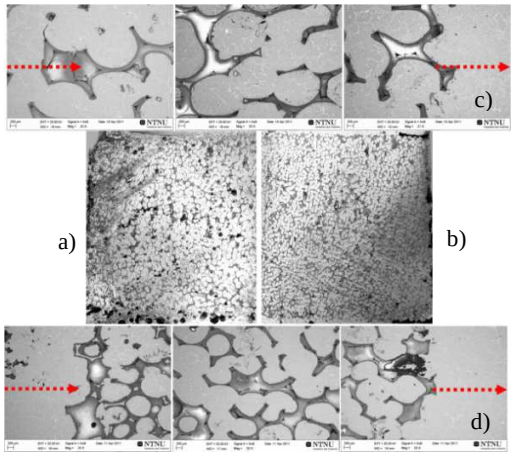

Figure 5. Fully primed and well wetted filters were obtained after 3 minutes of electromagnetic stirring, for (a) 50 PPI and for (b) 80 PPI CFFs, shown as half filter sections (50 mm thick and 50 mm radius). Complete gas removal was obtained after 10 minutes of electromagnetic stirring for c) 50 PPI and d) 80 PPI CFFs. The arrows represent the flow direction of the melt.

Filter productivity

It had been assumed that more efficient removal of gas would leave more of the interstitial volume of the CFFs available for flow, reducing the internal liquid velocity and pressure drop during filtration. Lower pressure drop would lead to increased productivity for any applied metal head during subsequent gravity filtration. The gravity filtration productivity, when using ~150 mm metal head has been plotted in Figure 6 for 30 PPI (gravity and EM primed) and 50 PPI filters (EM primed). Results indicate that both the EM primed 30 and 50 PPI filters had 25% more throughput than a gravity primed 30 PPI CFF. The high initial discharge rate for the 50 PPI filter was not maintained past 10 kg, due to the build up of 'cake' pressure drop. A very high loading of inclusions was used, such that each kg of metal filtered was equivalent to approximately 4 mt of typical industrial quality metal [5].

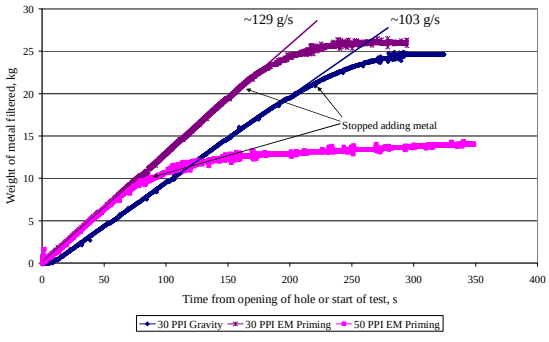

Figure 6. Impact of electromagnetic priming on filter productivity using ~150 mm of metal head for 30 PPI filters with and without EM priming, and a 50 PPI filter with EM priming. The EM primed 50 PPI filter had the same initial discharge rate as the 30 PPI EM primed and had a 25% greater discharge rate than the 30 PPI with gravity priming.

Efficiency of inclusion removal during gravity filtration after electromagnetic priming appeared to behave like conventional gravity filtration after gravity priming, once the increased superficial velocity was accounted for [5]. With electromagnetic priming, higher velocities were obtained as indicated in Figure 6 for a fixed metal head, and therefore slightly lower filtration efficiencies resulted.

Flow Field Modeling

In order to better understand the impact of the electromagnetic fields on priming, 2D axial symmetric FEM, using the commercial COMSOL® 4.2a code, were used to solve for steady state flow field solutions. Results are described in more detail elsewhere [5].

In Figure 7, the velocity field during the initial phase of the priming process is shown. The priming process begins with no metal and hence no Lorentz forces inside of the CFFs, greatly enhancing the curl, and creating substantial pressure gradients. The velocity magnitude is marked in Figure 7 with red arrows, and is estimated to be up to ~100 times higher than the typical industrial casting velocity as indicated in Table I [11].

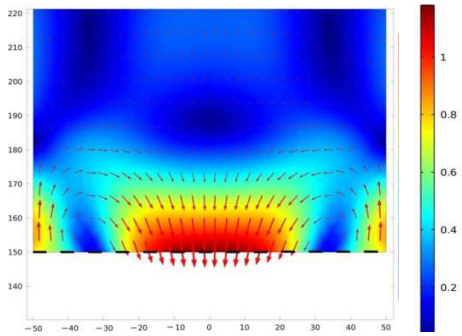

Figure 7. Initial induced flow field at during filter priming, showing the velocity field induced in the metal above the filter [m/s]. Metal is being continuously added to maintain the total metal head and is flowing 'out' at the bottom, i.e. filling the porous media of the ceramic filter [14].

Table I. Industrial Casting Velocity, Metal Flux and PPI Range for Different Casting Applications [11]

Type of Casting	Superficial Velocity mm/s	Metal Flux kg/s/m^2	Typical Pore Range
Billet	8-15	19-36	30-40
Slag	7-12	17-29	40-65
Continuous	2.5-8	6-19	20-50

After complete metal filling of the experimental apparatus shown in Figure 1 and 2, a very different flow pattern emerges. Current and hence Lorentz forces are now generated within the filter media and an upward metal flow is produced as indicated in Figure 8 for 30-80 PPI filters [5]. The upward flowing metal progressively removes gas trapped within the filter, as shown previously in Figure 5.

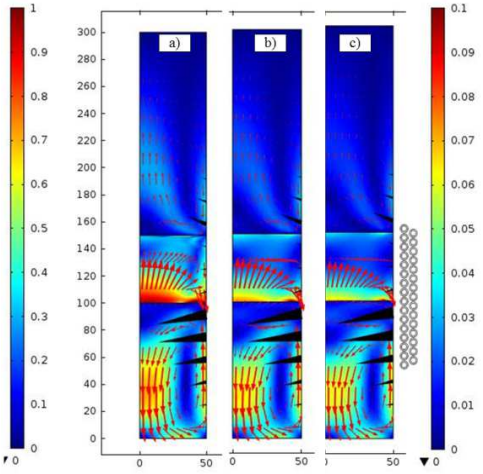

Figure 8. Flow fields calculated for (a) 30, (b) 50 and (c) 80 PPI filters, velocities scales indicated in m/s, left-hand scale is for metal regions, and the right-hand scale is for porous media regions. Position of induction coil is shown. Peak velocities in metal: 0.71, 0.64 and 0.64 m/s and in the filter: 0.19, 0.15 and 0.13 m/s, respectively. Conical arrows indicate relative Lorentz force strength (RMS). Regular arrows indicate direction and magnitude of fluid flow in metal and porous media regions, sizes are not comparable between regions [5].

Filtration Efficiency Modeling

The filtration efficiency is defined based on particle counts (either total or grouped into suitable size ranges):

$$E = \frac{N_i - N_o}{N_i} \qquad [2]$$

Where N_{in} is the count of particles entering into the filter per unit time, and N_{out} is the count of particles out of the filter per unit time.

Filtration efficiency can be empirically modeled using relatively simple models such as the one introduced by Iwasaki in 1937 [15]. Iwasaki defined the initial filtration efficiency E_0 (i.e. prior to the accumulation of significant particulates) using an initial filter coefficient λ_0 [mm^{-1}]:

$$E_0 = 1 - \exp^{-\lambda_0 L} \qquad [3]$$

Where L is the filter thickness [mm]. For most commercial CFFs, L has a magnitude of ~50 mm.

A slightly modified version of Iwasaki's equation was adopted by Apelian *et al.* [16] for the modeling of aluminum filtration, which accounts explicitly for superficial velocity.

$$E_0 = 1 - \exp^{-\frac{K_0 L}{u_s}} \quad [4]$$

Where E_0 is the initial filtration efficiency [unitless], u_s the velocity [mm/s] and K_0 was defined by Apelian as the initial 'kinetic' parameter [s^{-1}]. Apelian found that while K_0 increases with velocity, that the overall filtration efficiency decreases with higher velocity. The observation of reduced filtration efficiency at higher velocity has been verified in subsequent investigations using CFFs [11, 17, 18], as well as in the current study using SiC [5].

Examining Equation [4] it is clear that filtration efficiency should improve with thicker filters. Filters deeper than 50 mm are probably not currently applied due to the difficulty in priming such filters. With electromagnetic filtration filters as thick as 150 mm have already been primed using less than commercial priming heights as discussed previously.

K_0 in Equation [4] is an empirical value, which is particular to each type or grade of filter, and related to the physical characteristics of the particles being filtered (size, wetting, shape, etc.). K_0 values are expected to be higher for filters of higher PPI grade. Industrially determined K_0 values taken from LiMCA (Liquid Metal Cleanliness Analyzer) data for 30 and 50 PPI filters have been used to explore the sensitivity of filtration efficiency to velocity, thickness and filter type using Equation 4 [11]. The original K_0 values of Ray *et al.* have been adjusted to be in accordance with the use of superficial velocity in Equation [4] as shown in Table II.

Table II. K_0 Values for Pseudo-interstitial Velocity [11] and Superficial Velocity for 30 and 50 PPI CFFs

Size Group	30 PPI CFF	50 PPI CFF	30 PPI CFF	50 PPI CFF
	Pseudo-interstitial K_0 from literature [11]		Superficial corrected K_0	
15-20 µm	0.205	0.301	0.164	0.241
20-25 µm	0.250	0.360	0.200	0.288
25-30 µm	0.283	0.429	0.226	0.343
30-35 µm	0.323	0.478	0.258	0.382
35-40 µm	0.375	0.547	0.300	0.438
40-45 µm	0.409	0.627	0.327	0.502
45-50 µm	0.452	0.783	0.362	0.626
50-55 µm	0.509	0.940	0.407	0.752
55-60 µm	0.596	1.100	0.477	0.880
60+ µm	0.725	1.350	0.580	1.080

The impact of superficial velocity on filtration efficiency can be estimated using the adjusted K_0 values from Table II and Equation [4], as shown for both 30 and 50 PPI CFFs in Figure 9 for the industry standard 50 mm filter thickness as functions of particle size. The base case superficial velocity of 7.3 mm/s is equivalent to the 9.1 mm/s pseudo-interstitial velocity of Ray *et al.* [11]. Velocities covering a similar range to those shown in Table I have been selected. The estimated filtration efficiencies plotted in Figure 9 suggest that very high efficiency (>80%) can be obtained even for small 15-20 µm particles provided the filters are operated with a low enough velocity for 30 PPI filters. This would imply that filters of large area would be required to maintain productivity at such a low superficial velocity.

Figure 9 implies that a 50 PPI filter should be able to operate at significantly higher throughput (e.g. 7.3 vs. 5 mm/s) and achieve similar filtration efficiencies than a 30 PPI. At the same filtration velocity, about 10-20% higher filtration efficiency is achieved.

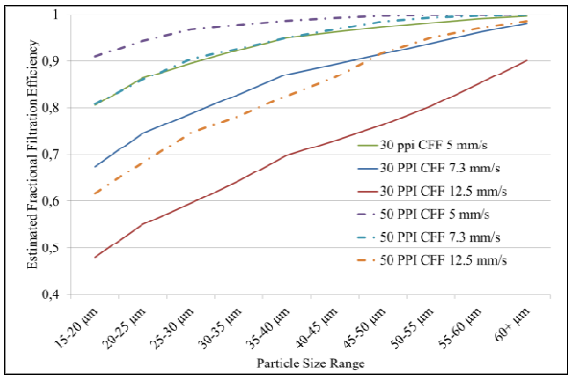

Figure 9. Estimated fractional filtration efficiency vs. particle size from 15 to >60 µm, for different superficial velocities using 50 mm thick 30 PPI CFFs (continuous lines) and 50 PPI CFFs (dotted lines).

An alternative to a very large filter area, is thicker filters to achieve similar high efficiencies. The impact of alternate thicknesses on filter performance is explored in Figure 10 for 30 PPI filters using the base case filtration velocity of 7.3 mm/s.

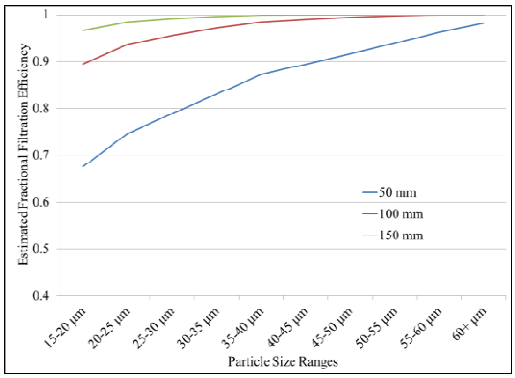

Figure 10. Estimated fractional filtration efficiency vs. particle size from 15 to >60 µm for three different filter thicknesses from 50-150 mm using 30 PPI CFFs.

Approximately 90% filtration efficiency can be obtained at the default 7.3 mm/s filtration velocity using 100 mm or thicker 30 PPI filters, representing an improvement of over 20%.

Filter Pressure Drop

If the option of thicker filters is to be applied, it is also necessary to calculate the metal head required to sustain the desired superficial velocity. The pressure gradient over the CFF can be estimated using the Forchheimer equation, as shown in Equation [5].

$$\frac{\Delta P}{L} = \frac{\mu}{k_1} u_s + \frac{\rho}{k_2} u_s^2 \qquad [5]$$

where ΔP is the pressure drop [Pa], L is the filter thickness [m], u_s is the fluid superficial velocity [m/s], μ is the fluid dynamic viscosity [Pa·s], ρ is the fluid density [kg/m^3], k_1 [m^2] and k_2 [m] are empirical constants called the Darcian and non-Darcian permeability coefficients. Recommended values for k_1 and k_2 are shown in Table III [7].

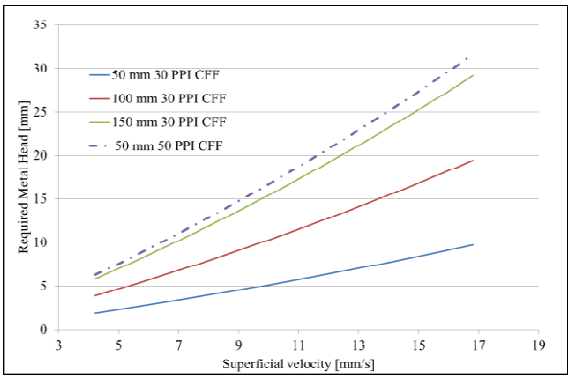

Figure 11. Metal head required to sustain flow as a function of superficial velocity, u_s shown in [mm/s] and filter thickness, L shown in [mm] from Equation [5], for 30 and 50 PPI filters.

A comparison of Figure 3 and Figure 11, indicates that much higher metal heads are required to prime than to sustain flow after priming, even assuming much thicker, e.g. 150 mm filters, than applied in industry today. An opportunity exists to apply electromagnetic priming to stacks of filters in existing filter box installations to prime 2 or 3 standard thicknesses of 50 mm filters and achieve higher filtration efficiencies, as indicated by the estimates shown previously in Figure 10.

Alternatively electromagnetic priming can be used to prime and enhance the productivity of higher grade, e.g. 50 PPI filters, which achieve improved filtration performances over 30 PPI as shown previously in Figure 9. Figure 11, indicates the required pressure drop to maintain flow for such a filter, verifying that priming head and not pressure drop during filtration is likely the factor determining usage.

Table III. Darcian K_1 and Non-Darcian K_2 Values for calculating the metal head regarding the superficial velocity for 30 and 50 PPI CFFs using the Forchheimer equation [7].

Filter Type (PPI)	Eq. 5 Forchheimer k_1 (m^2)	Eq. 5 Forchheimer k_2 (m)
30	5.08E-08	5.46E-04
40	3.10E-08	3.38E-04
50	1.57E-08	1.66E-04
80	6.52E-09	1.15E-04

Conclusions

Electromagnetic priming has been demonstrated to prime CFFs with less than the industry standard metal heads. The required metal head for electromagnetic priming of high PPI CFFs (50 and 80) was ~1/3rd of the standard height as published previously for industry. Furthermore, using electromagnetic priming, stacks of up to 3 filters have been primed using the same low metal heads.

The maximum allowable metal height in filter boxes currently dictates the type of filters and filtration rates that can be applied in industry. Based on the analysis of the filter permeability, it is the priming height and not the pressure drop during casting, which should typically limit the type of filter applied. Electromagnetic priming should allow higher PPI filters to be applied in existing filter bowls, than could otherwise be applied.

Furthermore the more efficient removal of gas from the CFFs should allow for lower metal height during filtration for a given throughput or a higher throughput for a given metal height. This may also make it practical to use for example 50 PPI filters with more consistent filtration performance to replace 30 PPI filters.

Improved melt quality can be achieved either by the use of higher PPI filters, lower velocities (and hence larger filtration areas) or thicker filters. With the use of electromagnetic priming both thicker filters and higher PPI filters become practicable for existing filter boxes.

Future Work

Experimental trials will be conducted to electromagnetically prime a stack of 3, 30 PPI grade CFFs. Lower grade CFFs may also be tested, e.g. 10 or 20 PPI. Gravity filtration experiments will be conducted to determine the filtration efficiency and verify the estimates given in Figures 9-10. Furthermore the application of an electromagnetic field to prime standard sized filters will be demonstrated in slightly modified industry standard filter boxes.

Acknowledgements

The present study was carried out as part of the RIRA (Remelting and Inclusion Refining of Aluminium) project funded by the Norwegian Research Council (NRC) - BIP Project No. 179947/I40. The industrial partners involved in the project are: Hydro Aluminium AS, SAPA Heat Transfer AB, Alcoa Norway ANS, Norwegian University of Science and Technology (NTNU) and SINTEF Materials and Chemistry. The funding granted by the industrial partners and the NRC is gratefully acknowledged.

The authors also wish to express their gratitude to Egil Torsetnes at NTNU for helping with the design and construction of the experimental apparatus. Sincere gratitude is also due to Kurt Sandaunet and Arne Nordmark of SINTEF for their support and help, as well as for the use of the SINTEF casting laboratory.

References

1. D. E. Groteke, "The Reduction of Inclusions in Aluminum by Filtration," Modern Casting, vol. 73, (1983), 25-27.
2. K. Butcher and D. Rogers, "Update on the Filtration of Aluminum Alloys with Fine Pore Ceramic Foam," Light Metals, (1990), 797-803.
3. M. W. Kennedy, S. Akhtar, J. A. Bakken and R. E. Aune, "Electromagnetically Enhanced Filtration of Aluminum Melts," Light Metals, (2011), 763-768.
4. R. Fritzsch, M. W. Kennedy, S. Akhtar, J. A. Bakken and R. E. Aune, "Electromagnetically Modified Filtration of Liquid Aluminium with a Ceramic Foam Filter," Accepted for Journal of Iron and Steel Research International, (2012), 1-4.
5. M. W. Kennedy, R. Fritzsch, S. Akhtar, J. A. Bakken and R. E. Aune, "Electromagnetically Modified Filtration of Aluminum Melts Part II: Filtration Theory and Experimental Filtration Efficiency with and without Electromagnetic Priming for 30, 50 and 80 PPI Ceramic Foam Filters," To be submitted to Metallurgical Transactions B, (2012), 1-69.
6. M. W. Kennedy, R. Fritzsch, S. Akhtar, J. A. Bakken and R. E. Aune, "Apparatus and Method for Priming a Molten Metal Filter," U.S. Patent Application, (2012), 1-26.
7. M. W. Kennedy, K. Zhang, R. Fritzsch, S. Akhtar, J. A. Bakken and R. E. Aune, "Characterization of Ceramic Foam Filters used for Liquid Metal Filtration," To be submitted to Metallurgical Transactions B, (2012), 1-46.
8. M. W. Kennedy, S. Akhtar, J. A. Bakken and R. E. Aune, "Analytical and Experimental Validation of Electromagnetic Simulations Using COMSOL®, re Inductance, Induction Heating and Magnetic Fields," COMSOL Conference 2011, Stuttgart, Germany, (2011), 1-9.
9. M. W. Kennedy, S. Akhtar, J. A. Bakken and R. E. Aune, "Analytical and FEM Modeling of Aluminum Billet Induction Heating with Experimental Verification," Light Metals, (2012), 269-275.
10. M. W. Kennedy, S. Akhtar, J. A. Bakken and R. E. Aune, "Improved Short Coil Correction Factor for Induction Heating of Billets," 3rd International Symposium on High-Temperature Metallurgical Processing, (2012), 373-382.
11. S. Ray, B. Milligan and N. Keegan, "Measurement of Filtration Performance, Filtration Theory and Practical Applications of Ceramic Foam Filters," Aluminium Cast House Technology, (2005), 1-12.
12. J. E. Dore and C. Bickert, "A Practical Guide on How to Optimize Ceramic Foam Filter Performance," Light Metals, (1990), 791-796.
13. N. Keegan, W. Schneider and H. P. Krug, "Evaluation of the Efficiency of Fine Pore Ceramic Foam Filters," Light Metals-Warrendale, (1999), 1-10.
14. R. Fritzsch, "Filtration of Aluminium Melts using Ceramic Foam Filters (CCF) and Electromagnetic Field," Trondheim: NTNU, Norway, (2011), 1-86.
15. T. Iwasaki, J. Slade and W. E. Stanley, "Some Notes on Sand Filtration [with Discussion]," Journal of American Water Works Association, vol. 29, (1937), 1591-1602.
16. D. Apelian and R. Mutharasan, "Filtration: A Melt Refining Method," Journal of Metals, vol. 9, (1980), 14-19.
17. C. Conti and P. Netter, "Deep Filtration of Liquid Metals: Application of a Simplified Model Based on the Limiting Trajectory Method," Separations Technology, vol. 2, (1992), 46-56.
18. H. Duval, C. Rivière, É. Laé, P. Le Brun and J. B. Guillot, "Pilot-Scale Investigation of Liquid Aluminum Filtration through Ceramic Foam Filters: Comparison between Coulter Counter Measurements and Metallographic Analysis of Spent Filters," Metallurgical and Materials Transactions B, vol. 40, (2009), 233-246.